

Commensurate structure of $\text{Ca}_2\text{CoSi}_2\text{O}_7$, a new
twinned orthorhombic structureKenji Hagiya,^{a*} Katsuhiko
Kusaka,^a Masaaki Ohmasa^a and
Kazuaki Iishi^b^aDepartment of Life Science, Himeji Institute of
Technology, Japan, and ^bDepartment of Chem-
istry and Earth Sciences, Yamaguchi University,
JapanCorrespondence e-mail:
hagiya@sci.himeji-tech.ac.jpReceived 4 January 2001
Accepted 12 January 2001

The crystal structure of the commensurate phase of $\text{Ca}_2\text{CoSi}_2\text{O}_7$, dicalcium cobalt disilicate, has been derived from the modulated structure described in $(3 + 2)$ -dimensional space. The structure is orthorhombic $P2_12_12$; $a = 23.510(4)$, $b = 23.510(4)$, $c = 5.025(1)$ Å (at 170 K), $Z = 18$. Since the crystal is twinned and the apparent diffraction symmetry is $4/mmm$, the parameters were refined by a newly developed least-squares program for the refinement of twinned crystals. The structure is essentially similar to the known structure of the melilite group, but with regular arrangement of the bundles along $[001]$ formed with four arrays of the sixfold coordinated Ca polyhedra and an array of CoO_4 tetrahedra. The distribution of the bundles found in the present structure is different from that reported by Riester *et al.* [(2000), *Z. Kristallogr.* **215**, 102–109].

1. Introduction

The crystal structure of the melilite group $\text{Ca}_2(\text{Mg,Al,Si})_3\text{O}_7$ was originally determined by Warren (1930). The structure of the tetragonal space group $P4_2/m$ is constructed from layers of the tetrahedral group $\{(\text{Mg,Al,Si})_3\text{O}_7\}^{4-}$ accommodating the larger Ca cations halfway between adjacent layers. Incommensurate modulation of the structure and its transition to the non-modulated structure [the normal (N) phase] at 358 K have been discovered by Hemingway *et al.* (1986) in synthetic åkermanite, an Mg end-member $\text{Ca}_2\text{MgSi}_2\text{O}_7$ of the melilite group. The incommensurate modulation and phase transition have also been found in $\text{Ca}_2(\text{Mg,Fe})\text{Si}_2\text{O}_7$ by Seifert *et al.* (1987) independently. Many incommensurate structures have been found thereafter in synthetic compounds of the group with various combinations of the elements (Röthlisberger *et al.*, 1990). The structure of the incommensurate phase was first determined for the cobalt analogue $\text{Ca}_2\text{CoSi}_2\text{O}_7$ of the group (Hagiya *et al.*, 1993). The incommensurate modulation of the structure is mainly ascribed to rotations and deformations of the tetrahedral units of the layers that cause variation of the coordination numbers of Ca atoms from six- to eightfold. A variety of coordination numbers of Ca has also been found in the other compounds of the group (Kusaka *et al.*, 1998; Bagautdinov *et al.*, 2000; Kusaka *et al.*, 2001). Four arrays of sixfold coordinated Ca—O polyhedra surrounding a central array of CoO_4 tetrahedra form a bundle along $[001]$ and many of those bundles are distributed in incommensurate structures so as to form octagons in the (001) projection of the structure (Kusaka *et al.*, 1998).

The phase transition of incommensurate $\text{Ca}_2\text{CoSi}_2\text{O}_7$ to a nearly commensurate phase with the magnitude of the primary modulation wavevector ($q = 0.324$) has been initially described by Riester & Böhm (1997) at around 160 K. The phase transition is accompanied by a remarkable hysteresis of q . They also presented a structure model assuming $q = 1/3$ (Riester *et al.*, 2000). Although the Laue class of the diffraction data was $4/mmm$, they assigned the space group $P\bar{4}$ to the structure based on the violation of the extinction rule, $P-2_1-$, and interpreted that the high diffraction symmetry is caused by the presence of twinning in the crystal. During the high-temperature studies of the incommensurate phase (IC phase) of $\text{Ca}_2\text{CoSi}_2\text{O}_7$, Kusaka (1999) found that the hysteresis reported by Riester & Böhm (1997) is observable in the whole stability range of the incommensurate phase and the q value varies from 0.286 (at 468 K) to $1/3$ (below 242.3 K). A computer program was then developed to study variations of long-range order in the incommensurate phase associated with the change of q (Kusaka, 1999). Using the amplitudes of the modulation waves determined at 297 K and the symmetry operations of the incommensurate structure, he has constructed various structures of the incommensurate phase for the required q values in the three-dimensional space, and found that eight bundles form octagons in the structure and various arrangement of the octagons are realised in the structures for different q values. This suggests that the formation of the octagonal arrangement of the bundles should play an important role in holding the long-range order of the structure.

The method was also applied to the commensurate phase with $q = 1/3$ and assuming the space group to be $P\bar{4}$. The simulated structure is almost the same as the structure reported by Riester *et al.* (2000). However, since the present diffraction studies at low temperature indicated that the extinction rule derived from 2_1 axes should not be violated, a new structure was constructed with $q = 1/3$, the modulation amplitudes determined at 297 K and the orthorhombic space group $P2_12_12_1$. The structure has been successfully refined and the determined structure is different from that given by Riester *et al.* (2000). This paper reports the new orthorhombic

structure, which gives a different ordering scheme of the bundles from the reported model (Riester *et al.*, 2000).

2. Experimental

The sample used for the determination of the q values at various temperatures was synthesized by a floating-zone (FZ) method to prevent contamination of the specimen. The crystal was ground in a spherical form ($r = 0.135$ mm) to avoid errors of absorption corrections. X-ray diffraction was measured by a CAD-4 diffractometer (Enraf–Nonius) on which a gas-flow heating system developed in our laboratory was installed, and by another CAD-4 diffractometer with a liquid N_2 gas-flow cooling system (Rigaku Co. Ltd) and a cassette for imaging plates. Imaging plates were used to check the Laue class and reflection conditions by long exposures. The intensity data were corrected for the Lorentz, polarization and absorption factors.

The cell parameters and setting parameters of the basic cell of the specimen were determined with angular data of 25 main reflections in the temperature range 96–493 K ($T_{\text{IC-N}}$). The cell parameters were refined using the least-squares program *CELDIM* in the *MolEN* system (Fair, 1990). After determination of the cell parameters and setting parameters, peak profiles of the satellite reflections were measured with the ω - 2θ scan mode to observe the variation of the q values and also the appearance and disappearance of satellites in the entire temperature range. The observed variation of the q values *versus* temperature change is depicted in Fig. 1. The hysteresis of q described at the transition between the commensurate and incommensurate phases (Riester & Böhm, 1997) is observable in the whole stability range of the incommensurate phase. On cooling, a new peak at $q = 0.333$ (1) appeared beside the satellite reflection at 242.3 K, as indicated in Fig. 2, while on heating the q value jumps discontinuously from 0.332 (1) to 0.310 (1) in the temperature range between 278.6 and 283.0 K and the similar coexistence of peaks of the two phases was not ascertained.

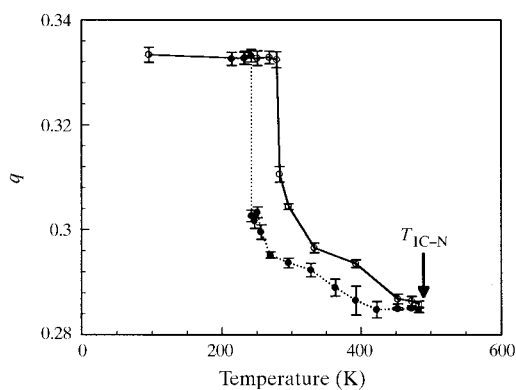


Figure 1
Variation in the magnitude q of the incommensurate primary modulation wavevectors *versus* temperature change. The arrow indicates the temperature $T_{\text{IC-N}}$.

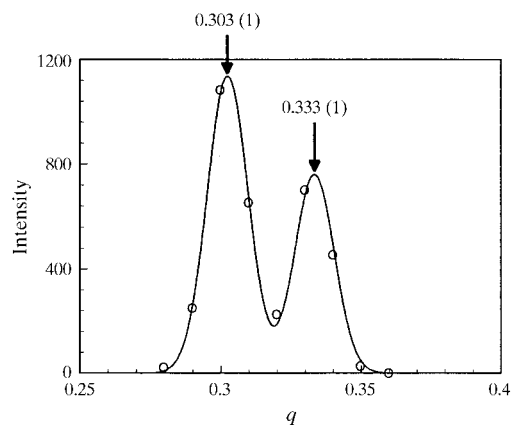


Figure 2
Profile of the satellite reflection 34001 of the incommensurate phase at 242.3 K. The reflection of the commensurate phase corresponding to 34001 is also observed. The arrows indicate the q values of the satellites.

Table 1
Experimental details.

Crystal data	
Chemical formula	Ca ₂ CoSi ₂ O ₇
Chemical formula weight	307.26
Cell setting, space group	Orthorhombic, <i>P</i> 2 ₁ 2 ₁ 2
<i>a</i> , <i>b</i> , <i>c</i> (Å)	23.510 (4), 23.510 (4), 5.025 (1)
<i>V</i> (Å ³)	2777 (1)
<i>Z</i>	18
<i>D_x</i> (Mg m ⁻³)	3.307
Radiation type	Mo <i>K</i> α
No. of reflections for cell parameters	25
θ range (°)	11–32
μ (mm ⁻¹)	4.77
Crystal form, colour	Sphere, blue
Crystal radius (mm)	0.135
Data collection	
Diffractometer	Enraf–Nonius CAD-4
Absorption correction	Analytical
<i>T</i> _{min}	0.418
<i>T</i> _{max}	0.446
No. of measured, independent and observed parameters	8374, 6342, 6152
Criterion for observed reflections	<i>I</i> > 1.5σ(<i>I</i>)
<i>R</i> _{int}	0.019
Range of <i>h</i> , <i>k</i> , <i>l</i>	0 → <i>h</i> → 33 0 → <i>k</i> → 46 0 → <i>l</i> → 10
Refinement	
Refinement on	<i>F</i> ²
<i>R</i> [<i>F</i> ² > 1.5σ(<i>F</i> ²)], <i>wR</i> (<i>F</i> ²), <i>S</i>	0.084/0.139/1.210
No. of reflections and parameters used in refinement	6152, 217
Weighting scheme	1/[σ ² (<i>F</i> _o ²) + 0.81 <i>F</i> _o ² + 0.004 <i>F</i> _o ⁴]

The Laue class of the commensurate phase was assigned to *4/mmm*, because deviation from *4/mmm* was not detected from the intensity distribution measured by a scintillation counter and an imaging plate. The reflection conditions of *h*00 and *0k*0 reflections were then examined. Very weak intensities were detected at 900, 090, 27,00 and 0,27,0 by measurements with a CAD-4 diffractometer. The first two reflections were considerably stronger than the next two. However, 900 and 090 were not visible in the diffraction pattern recorded on the heavily exposed imaging plate (IP). Using the same method we found very weak reflections undetected by the scintillation counter (Kusaka *et al.*, 2001). 27,00 and 0,27,0 were outside the recorded area in the present study. Since the diffraction condition of the measurements employed for the exposure with the IP was different from that adopted for the diffraction by CAD-4 and the stronger reflections 900 and 090 were not detected with the IP, we assumed that the weak intensities observed at the above four reflections should be caused by multiple diffraction effects and the reflection condition derived from the screw axis should not be violated. Thus, the diffraction condition was deduced to be *P*-2₁- for the present material, which led us to the same space group *P*4₂*1m* of melilite. However, the results of the least-squares refinements with the single-crystal model (*P*4₂*1m*) did not converge and some of the thermal displacement parameters became very high (one with *B* > 10). The high Laue symmetry

should be apparent resulting from twinning of two types of domains referred by {110} mirror planes of the tetragonal cell and may be induced in the crystal during the phase transition. The possible space group of the commensurate phase is therefore assigned to *P*2₁2₁2 and the apparent high symmetry of the Laue class suggests that the volumes of the twins are equal. The crystal data and the conditions of the measurements are listed in Table 1.

3. Construction of the structure

A series of studies has been carried out to investigate variations of the incommensurate structure of Ca₂CoSi₂O₇ with changes in *q* values (Kusaka, 1999). The method employed for the studies is briefly described below.

Diffraction patterns of the incommensurate phase of Ca₂CoSi₂O₇ indicate that each main reflection is surrounded by eight satellites and the Laue classes for both main and satellite reflections are *4/mmm* and the modulation is two-dimensional with the two wavevectors **k**₁ = *q*(**a*** + **b***) and **k**₂ = *q*(-**a*** + **b***). Then all reflections were indexed with five integers and five base vectors which are related to the three crystallographic axes and the two wavevectors [**h** = *h***a*** + *k***b*** + *l***c*** + *m***k**₁ + *n***k**₂; **a***, **b*** and **c*** are the base vectors of the reciprocal lattice of the basic cell (the unit cell derived from the main reflections)]. Thus, the whole reflections are described in the (3 + 2)-dimensional reciprocal space (de Wolff, 1974) with indices *hklmn*, where the multiplied integers *mn* = 0 or ±1.

Since the modulation in the structure is caused only by shifts of the atoms from the mean positions (the positions in the basic structure determined only with main reflections), an atomic position vector **x** of the modulated structure in the three-dimensional space is written as

$$\mathbf{x}_j = \mathbf{n} + \bar{\mathbf{x}}_j + \mathbf{u}_j,$$

where **n** is a lattice vector of the basic cell, $\bar{\mathbf{x}}_j$ a position vector of an atom in the basic cell and **u**_{*j*} a displacement vector of the atom determined in (3 + 2)-dimensional space. **u**_{*j*} is expanded in a Fourier series. As up to the first-order satellites are observed in the diffraction patterns and the modulation is a two-dimensional one, displacement *u*_{*ij*}(*q*) (*i* = 1, 2, 3 corresponding to *x*, *y*, *z*) of the *j*th atom can be expressed as

$$u_{ij}(q) = \sum_m \sum_n [A_{ij}^{mn}(q) \cos 2\pi(mt_1 + nt_2) + B_{ij}^{mn}(q) \sin 2\pi(mt_1 + nt_2)], \quad (1)$$

where *q* is the magnitude of the modulation wavevectors, *A*_{*ij*}^{*mn*}(*q*) and *B*_{*ij*}^{*mn*}(*q*) are Fourier amplitudes of the displacement determined for *q*, and *t*₁ and *t*₂ are phases of the modulation at the atomic position **n** + $\bar{\mathbf{x}}_j$. Based on a simple consideration, we can conclude that the intensity of the satellite *I*_{*n*} is proportional to the square of the Fourier amplitudes of the modulation waves, when |*A*_{*ij*}^{*mn*}(*q*)| ≪ 1 and |*B*_{*ij*}^{*mn*}(*q*)| ≪ 1 (Kusaka, 1999).¹ The amplitudes of the modulation waves

¹To be published elsewhere.

determined at 297 K are of the order 10^{-3} and suggest that the proportionality between the observed structure factors of the satellite reflections and the amplitudes of the modulation waves should be satisfied. As the determinations of the structures of the incommensurate phase at different temperatures clarified that a linear correlation between structure factors of satellites and the amplitudes of the modulation waves of the atoms is held for different q values, we may write the following relation between the satellite intensities and the amplitudes of the modulation waves for different q values (q and q_0)

$$A(q)/A(q_0) \simeq [I(q)/I(q_0)]^{1/2} = |F(q)|/|F(q_0)|.$$

Thus, (1) is rewritten as

$$u_{ij}(q) \simeq [|F(q)|/|F(q_0)|] \sum_m \sum_n [A_{ij}^{mn}(q_0) \cos 2\pi(mt_1 + nt_2) + B_{ij}^{mn}(q_0) \sin 2\pi(mt_1 + nt_2)]. \quad (2)$$

Therefore, coordinates of atoms in the modulated structure with an arbitrary q value can be given with the amplitudes of the modulation waves determined for q_0 and the ratio of the structure factors of the satellites for q and q_0 . A computer program was then developed (Hagiya & Kusaka, unpublished) to construct structures with arbitrary q values. Since the incommensurate structure determined with the intensity data measured at 468 K ($q = 0.289$) coincides well with the structure constructed by the program with the same q value and the Fourier amplitudes determined at 297 K ($q_0 = 0.2913$), and since the octagonal distribution of the bundles is identical in both structures, the program has been utilized for further

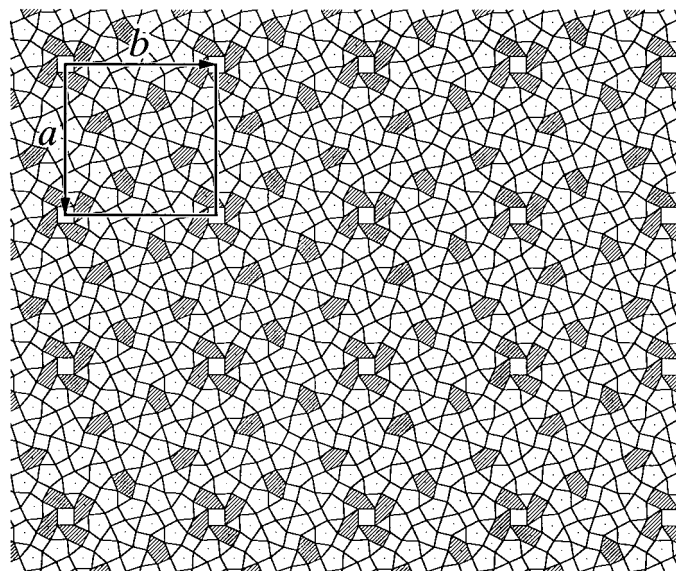


Figure 3
The constructed structure with the space-group symmetry $P\bar{4}$. Small squares indicate CoO_4 tetrahedra, and triangles and pentagons denote tetrahedra of Si and Ca—O polyhedra, respectively. The shaded pentagons correspond to the sixfold coordinated Ca—O polyhedra. The unit cell of the commensurate structure is indicated with the large square.

studies on the incommensurate structures of $\text{Ca}_2\text{CoSi}_2\text{O}_7$ (Kusaka, 1999).

4. Derivation and refinements of the structure

The transition between the incommensurate and commensurate phases of the present material may be regarded as a change of structure, keeping their averaged structures unchanged, because the apparent space groups and intensity distributions observed for the main reflections diffracted by these phases are equal. This fact implies that a commensurate structure can be described in $(3 + 2)$ -dimensional superspace as a variation of the incommensurately modulated structures having a rational q value ($q = 1/3$ in the present studies) and therefore its structure in three-dimensional space can be constructed by the process described in the preceding section from the modulation amplitudes for q_0 determined experimentally.

Since parameters of each atom in the $(3 + 2)$ -dimensional space are represented in a repeating unit spanned by the two-dimensional internal directions t_1 and t_2 , all the structural information of the incommensurate phase is enclosed in the whole area of the repeating unit (Bagautdinov *et al.*, 2000). However, information on a commensurate structure is only given at definite positions in the repeating unit owing to the commensurable relation between modulation waves and the basic cell edges. In the commensurate phase of $\text{Ca}_2\text{CoSi}_2\text{O}_7$, all information relating to the structure is localized at discrete positions in $(3 + 2)$ -dimensional space with the interval one third of the unit lengths of t_1 and t_2 . This results in different combinations between the origin of the three-dimensional basic cell and the initial phase in the (t_1, t_2) area, which generate different structures in the construction processes, and the most important problem is how to select an initial phase (t_1^0, t_2^0) for construction of the commensurate structure.

The structure with the space group $P\bar{4}$ (Fig. 3) was first constructed with $(0, 0)$ for the initial phase (t_1^0, t_2^0) at the origin of the basic cell, although the assigned reflection condition is not fulfilled. The initial coordinates of the atoms in the asymmetric unit were calculated using (2). The constructed figure indicates that the structure coincides well with that proposed by Rieger *et al.* (2000). The symmetry of the structure corresponding to the phase $(\frac{1}{2}, \frac{1}{2})$ is also $P\bar{4}$, but the structure is the mirror image [across $\{110\}$] of the structure derived with $(0, 0)$. The parameters of the structure were then refined by the least-squares program *HITLST* (Hagiya, unpublished), assuming that the structure is twinned. The refinements using the satellite reflections however gave no satisfactory agreement between the observed and calculated intensities, as indicated in Table 2. No improvement in R and wR was obtained by further refinements.

Then the structure was constructed with the phase $(\frac{1}{2}, 0)$ for (t_1^0, t_2^0) , which satisfies the symmetry $P2_12_12$ (Fig. 4). The initial coordinates of the atoms in the asymmetric unit were also calculated using (2). The structure parameters were refined by the same least-squares program *HITLST*, assuming twinning of the structure. Since the refinements with only the satellite

Table 2Results of the refinements for the structures $P\bar{4}$ and $P2_12_12$.

Space group Reflections used		$P\bar{4}$		All
		Satellites ^a	Satellites ^b	
For all 6152 reflections	<i>R</i>	0.284	0.109	0.084
	<i>wR</i>	—	—	0.139
For 789 main reflections	<i>R</i>	0.321	0.116	0.080
	<i>wR</i>	—	—	0.119
For 2703 satellites with <i>mn</i> = ± 1	<i>R</i>	0.145	0.082	0.088
	<i>wR</i>	0.123	0.073	0.138
For 2660 satellites with <i>mn</i> = 0	<i>R</i>	0.247	0.101	0.102
	<i>wR</i>	0.216	0.094	0.154
	<i>S</i>	—	—	1.210

Weighting schemes: ^a*w* = 1, ^b*w* = $1/[\sigma^2(F_o^2) + 0.81F_o^2 + 0.004F_o^4]$.

reflections gave satisfactory convergence, further refinements were carried out with all the independent main and satellite reflections. The agreement between the observed and calculated intensities was satisfactory (Table 2). The anisotropic temperature factors were not included in the refinements, because the reflections in the independent region of the Laue class *mmm* were not used for the refinements, but those in the independent region of *4/mmm* were used. The coordinates of the atoms and the isotropic temperature factors have been deposited.² The structure constructed with $(0, \frac{1}{2})$ also has the symmetry $P2_12_12$ and is also the mirror image of the structure constructed with $(\frac{1}{2}, 0)$ for (t_1^0, t_2^0) .

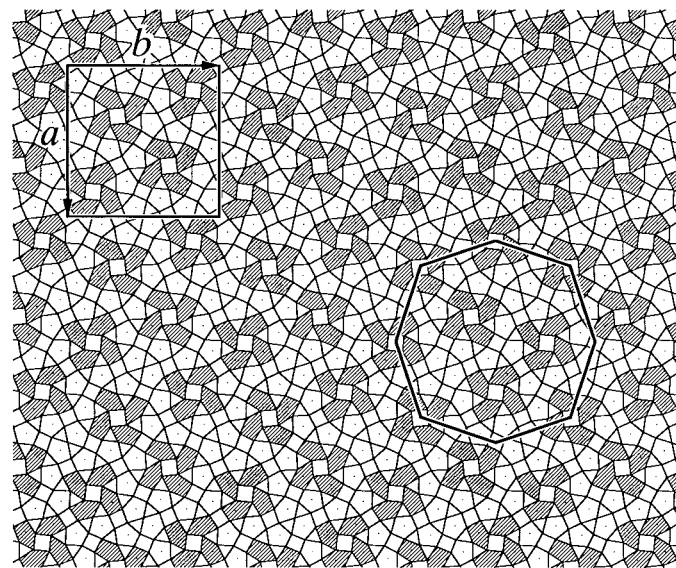
The commensurate structure can also be refined in $(3+2)$ -dimensional space, as for incommensurate structures. However, we refined the structure parameters in three-dimensional space, because the number of parameters for the refinements in three-dimensional space is equal to that for the refinements in $(3+2)$ -dimensional space.

5. Description of the structure

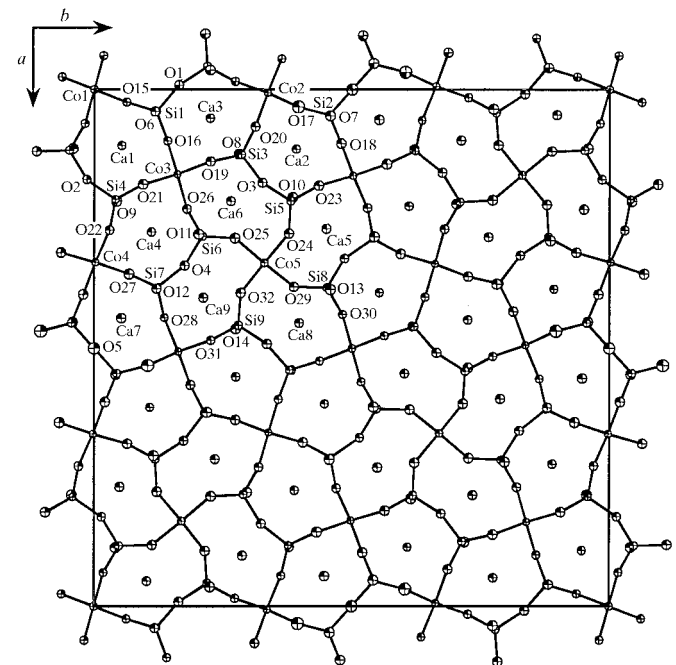
The interatomic distances together with the bond-valence values (Brown & Altermatt, 1985) estimated from each distance are given in Table 3. The mean Si—O distance of each tetrahedron ranges between 1.623 (5) and 1.635 (6) Å. Two SiO₄ tetrahedra form a dimer, Si₂O₇, and the dimers are connected with CoO₄ tetrahedra sharing their corners to form tetrahedral layers perpendicular to [001]. The distance between the Si and O atoms bridging the two Si atoms in a dimer is the longest Si—O distance (mean value for all Si tetrahedra: 1.667 Å) and the length between Si and the apical O atom is the shortest (mean value: 1.601 Å). These values coincide well with the corresponding distances (1.668 and 1.605 Å) of the dimer in rankinite (Ca₃Si₂O₇; Saburi *et al.*, 1976). The mean Co—O distances of the CoO₄ tetrahedra are in the range 1.945 (5)–1.958 (5) Å. The CoO₄ tetrahedra at the centres of the bundles (the tetrahedron of Co5) are very much flattened along [001] and the two independent angles intersecting the [001] direction being 124.4 and 124.2°, respectively,

² Supplementary data for this paper are available from the IUCr electronic archives (Reference: SN0009). Services for accessing these data are described at the back of the journal.

are much larger than the regular tetrahedral angle 109.47°. These features are also recognized as the features in the incommensurate structures of Ca₂CoSi₂O₇ and Ca₂(Mg_{0.55}Fe_{0.45})Si₂O₇ (Kusaka *et al.*, 1998). Ca atoms are located between the tetrahedral layers and are surrounded by eight O atoms. The Ca—O distances, however, vary widely and some of the polyhedra of Ca can be assigned to be of sixfold coordination (Ca5, Ca6, Ca8 and Ca9) and of sevenfold one (Ca2) when the distances longer than 2.9 Å are excluded. Three

**Figure 4**

The constructed structure with the space-group symmetry $P2_12_12$. The notation of each polygon is same as that given in Fig. 3. Part of the octagonal arrangement of the bundles is also outlined.

**Figure 5**

The structure of the commensurate Ca₂CoSi₂O₇ determined at 170 K.

Table 3
Interatomic distances (Å) and bond valences.

	Distances	Bond valence
Ca1—O2	2.753 (5)	0.120
Ca1—O6	2.517 (6)	0.226
Ca1—O9	2.851 (6)	0.092
Ca1—O13 ⁱ	2.519 (6)	0.225
Ca1—O15	2.398 (5)	0.312
Ca1—O16	2.531 (5)	0.218
Ca1—O21	2.436 (5)	0.282
Ca1—O30 ^l	2.419 (5)	0.295
Mean	2.553 (5)	Sum: 1.770
Ca2—O3	2.691 (5)	0.141
Ca2—O7	2.515 (6)	0.227
Ca2—O8	2.939 (6)	0.072
Ca2—O10	2.512 (6)	0.229
Ca2—O17	2.391 (6)	0.318
Ca2—O18	2.461 (5)	0.263
Ca2—O20	2.506 (5)	0.233
Ca2—O23	2.415 (5)	0.298
Mean	2.554 (6)	Sum: 1.781
Ca3—O1	2.615 (6)	0.174
Ca3—O6	2.841 (6)	0.094
Ca3—O8	2.446 (6)	0.274
Ca3—O14 ^h	2.504 (5)	0.235
Ca3—O16	2.617 (5)	0.173
Ca3—O19	2.399 (5)	0.311
Ca3—O20	2.523 (5)	0.223
Ca3—O31 ⁱⁱ	2.445 (5)	0.275
Mean	2.549 (5)	Sum: 1.759
Ca4—O4	2.705 (5)	0.136
Ca4—O9	2.448 (6)	0.273
Ca4—O11	2.476 (5)	0.253
Ca4—O12	2.872 (5)	0.087
Ca4—O21	2.632 (5)	0.166
Ca4—O22	2.372 (5)	0.335
Ca4—O26	2.411 (5)	0.301
Ca4—O27	2.575 (6)	0.193
Mean	2.561 (5)	Sum: 1.744
Ca5—O2 ⁱⁱⁱ	2.360 (5)	0.346
Ca5—O9 ⁱⁱⁱ	2.504 (6)	0.234
Ca5—O10	2.442 (6)	0.277
Ca5—O13	2.960 (6)	0.068
Ca5—O22 ⁱⁱⁱ	2.557 (5)	0.203
Ca5—O23	2.409 (5)	0.303
Ca5—O24	2.297 (5)	0.410
Ca5—O29	3.506 (5)	0.016
Mean	2.630 (5)	Sum: 1.857
Ca6—O3	2.427 (5)	0.288
Ca6—O8	2.458 (6)	0.265
Ca6—O10	3.007 (6)	0.060
Ca6—O11	2.429 (5)	0.287
Ca6—O19	2.500 (5)	0.237
Ca6—O24	3.511 (5)	0.015
Ca6—O25	2.316 (5)	0.389
Ca6—O26	2.463 (5)	0.262
Mean	2.639 (5)	Sum: 1.803
Ca7—O5	2.450 (5)	0.271
Ca7—O7 ^{iv}	2.858 (6)	0.090
Ca7—O7 ⁱ	2.551 (6)	0.206
Ca7—O12	2.459 (5)	0.265
Ca7—O17 ^{iv}	2.883 (6)	0.084
Ca7—O18 ⁱ	2.475 (5)	0.253
Ca7—O27	2.455 (6)	0.267
Ca7—O28	2.383 (5)	0.325
Mean	2.564 (6)	Sum: 1.761
Ca8—O1 ^{iv}	2.420 (6)	0.294

Table 3 (continued)

	Distances	Bond valence
Ca8—O6 ^{iv}	2.486 (5)	0.246
Ca8—O13	2.433 (6)	0.284
Ca8—O14	3.130 (5)	0.043
Ca8—O15 ^{iv}	2.421 (5)	0.293
Ca8—O29	2.300 (5)	0.407
Ca8—O30	2.425 (5)	0.290
Ca8—O32	3.434 (5)	0.019
Mean	2.631 (5)	Sum: 1.876
Ca9—O4	2.429 (5)	0.287
Ca9—O11	3.091 (5)	0.048
Ca9—O12	2.466 (5)	0.260
Ca9—O14	2.401 (5)	0.309
Ca9—O25	3.515 (5)	0.015
Ca9—O28	2.496 (5)	0.239
Ca9—O31	2.396 (5)	0.314
Ca9—O32	2.325 (5)	0.380
Mean	2.640 (5)	Sum: 1.852
Co1—O15 ^v	1.949 (5)	0.499
Co1—O15 ^{vi}	1.949 (5)	0.499
Co1—O30 ⁱⁱ	1.944 (5)	0.506
Co1—O30 ^l	1.944 (5)	0.506
Mean	1.947 (5)	Sum: 2.010
Co2—O17 ^v	1.944 (6)	0.506
Co2—O20	1.950 (5)	0.498
Co2—O28 ⁱⁱ	1.952 (5)	0.495
Co2—O31 ^{vii}	1.956 (5)	0.490
Mean	1.950 (5)	Sum: 1.989
Co3—O16 ^v	1.956 (5)	0.490
Co3—O19	1.962 (5)	0.482
Co3—O21	1.964 (5)	0.479
Co3—O26 ^v	1.950 (5)	0.498
Mean	1.958 (5)	Sum: 1.949
Co4—O18 ⁱ	1.947 (6)	0.502
Co4—O22	1.945 (5)	0.505
Co4—O23 ^{viii}	1.954 (5)	0.493
Co4—O27 ^v	1.961 (6)	0.483
Mean	1.952 (5)	Sum: 1.983
Co5—O24	1.937 (5)	0.516
Co5—O25 ^v	1.944 (5)	0.506
Co5—O29 ^v	1.948 (5)	0.501
Co5—O32	1.950 (5)	0.498
Mean	1.945 (5)	Sum: 2.021
Si1—O1 ^v	1.666 (6)	0.893
Si1—O6	1.606 (6)	1.050
Si1—O15 ^v	1.635 (5)	0.971
Si1—O16 ^v	1.614 (5)	1.027
Mean	1.630 (6)	Sum: 3.941
Si2—O5 ^{vii}	1.659 (3)	0.910
Si2—O7	1.596 (5)	1.079
Si2—O17 ^v	1.619 (7)	1.014
Si2—O18 ^v	1.616 (6)	1.022
Mean	1.623 (5)	Sum: 4.025
Si3—O3	1.675 (5)	0.871
Si3—O8 ^v	1.597 (6)	1.076
Si3—O19	1.646 (6)	0.942
Si3—O20	1.622 (5)	1.005
Mean	1.635 (6)	Sum: 3.894
Si4—O2	1.671 (5)	0.881
Si4—O9 ^v	1.596 (6)	1.079
Si4—O21	1.619 (6)	1.014
Si4—O22	1.627 (5)	0.992
Mean	1.628 (6)	Sum: 3.966

Table 3 (continued)

	Distances	Bond valence
Si5—O3	1.660 (5)	0.907
Si5—O10 ^v	1.607 (6)	1.047
Si5—O23	1.655 (6)	0.920
Si5—O24	1.613 (5)	1.030
Mean	1.634 (6)	Sum: 3.904
Si6—O4 ^v	1.666 (5)	0.893
Si6—O11	1.603 (6)	1.058
Si6—O25 ^v	1.608 (5)	1.044
Si6—O26 ^v	1.635 (5)	0.971
Mean	1.628 (5)	Sum: 3.966
Si7—O4 ^v	1.664 (5)	0.898
Si7—O12	1.601 (5)	1.064
Si7—O27 ^v	1.623 (6)	1.003
Si7—O28 ^v	1.625 (5)	0.997
Mean	1.628 (5)	Sum: 3.962
Si8—O2 ^{ix}	1.665 (5)	0.895
Si8—O13	1.598 (6)	1.073
Si8—O29 ^v	1.621 (6)	1.008
Si8—O30 ^v	1.638 (5)	0.963
Mean	1.631 (6)	Sum: 3.939
Si9—O1 ^{iv}	1.673 (6)	0.876
Si9—O14 ^v	1.601 (6)	1.064
Si9—O31	1.656 (5)	0.917
Si9—O32	1.609 (6)	1.041
Mean	1.635 (6)	Sum: 3.898

Symmetry codes: (i) $\frac{1}{2} - x, -\frac{1}{2} + y, 1 - z$; (ii) $-\frac{1}{2} + x, \frac{1}{2} - y, 1 - z$; (iii) $\frac{1}{2} - x, \frac{1}{2} + y, 1 - z$; (iv) $\frac{1}{2} + x, \frac{1}{2} - y, 1 - z$; (v) $x, y, -1 + z$; (vi) $-x, -y, -1 + z$; (vii) $-\frac{1}{2} + x, \frac{1}{2} - y, -z$; (viii) $\frac{1}{2} - x, -\frac{1}{2} + y, -z$; (ix) $\frac{1}{2} - x, \frac{1}{2} + y, -z$.

independent Ca atoms are described as sevenfold coordinated ones in rankinite (Saburi *et al.*, 1976), but one of them (Ca1) can be regarded as a sixfold coordination if the length longer than 2.9 Å is excluded. The mean bond-valence sum of Co is 1.99 and that of Si is 3.94. The mean value of the sums for the Ca atoms with sixfold coordination is 1.85 and slightly but distinctly higher than that for the other Ca atoms (1.76). Although the bond-valence sums estimated for Co and Si almost agree to their formal charges, the sums for Ca atoms are significantly lower than the expected formal charge and indicate that their sites are still too loose for Ca.

The structure determined (Fig. 5) is thus essentially similar to the known structure (Warren, 1930), but is characterized with the ordered arrangement of bundles of the same sixfold coordinated Ca atoms as in the incommensurate structures of the åkermanite group (Kusaka *et al.*, 1998, 2001). 28.5% of Ca atoms are sixfold-coordinated Ca in the incommensurate phase at 297 K, while 44.4% of Ca atoms are sixfold-coordinated in the commensurate structure and all of them form bundles. Four bundles are consequently included in each commensurate cell. The octagonal distribution of the bundles characterizing the incommensurate structure is not found in the commensurate phase, but many fractions of the octagons

(three quarters of an octagon) are scattered in the structure instead (Fig. 4). The feature of the structure constructed with the space group $P\bar{4}$ is quite different from the structure of $P2_12_12$: the number of sixfold-coordinated Ca is eight in the commensurate cell and only one bundle is included in the unit cell. Thus, only 22.2% of the calcium sites are sixfold coordinated and the number is less than that in the incommensurate structure. Many different commensurate structures with $q = 1/3$ can be constructed with the arbitrary initial phases (t_1^0, t_2^0) and they indicate various arrangements of the bundles, although the octagonal distribution is not realised. Almost all have the symmetry $P1$ and no systematic extinction is expected from the structure.

The structures with the initial phases $(0, 0)$ and $(\frac{1}{2}, 0)$ of the $(3 + 2)$ -dimensional space were constructed with $q = 0.324$ (q reported by Riester & Böhm, 1997) in order to compare them to the structures $P\bar{4}$ and $P2_12_12$ constructed with $q = 1/3$. The two structures with $q = 0.324$ are similar to each other, in which the greater part of the structure is similar to the structure of $P\bar{4}$ and the rest resembles the structure of $P2_12_12$. The averaged structure of these two parts may also be similar to the structure proposed by Riester *et al.* (2000).

The authors would like to thank Dr B. Bagautdinov of our laboratory for critical reading of the manuscript. The work was financially supported in part by a Grant-in-Aid for Scientific Research (B) (No. 07454135) from the Ministry of Education, Science and Culture, Japan, who are gratefully acknowledged.

References

- Bagautdinov, B., Hagiya, K., Kusaka, K., Ohmasa, M. & Iishi, K. (2000). *Acta Cryst.* **B56**, 811–821.
- Brown, I. D. & Altermatt, D. (1985). *Acta Cryst.* **B41**, 244–247.
- Fair, C. K. (1990). *MolEN*. Delft, The Netherlands.
- Hagiya, K., Ohmasa, M. & Iishi, K. (1993). *Acta Cryst.* **B49**, 172–179.
- Hemingway, B. S., Evans, H. T. Jr, Nord, G. L. Jr, Haselton, H. T. Jr, Robie, R. A. & McGee, J. J. (1986). *Can. Mineral.* **24**, 425–434.
- Kusaka, K. (1999). Ph.D. thesis. Himeji Institute of Technology, Japan.
- Kusaka, K., Hagiya, K., Ohmasa, M., Okano, Y., Mukai, M., Iishi, K. & Haga, N. (2001). *Phys. Chem. Miner.* In the press.
- Kusaka, K., Ohmasa, M., Hagiya, K., Iishi, K. & Haga, N. (1998). *Miner. J.* **20**, 47–58.
- Riester, M. & Böhm, H. (1997). *Z. Kristallogr.* **212**, 506–509.
- Riester, M., Böhm, H. & Petricek, V. (2000). *Z. Kristallogr.* **215**, 102–109.
- Röthlisberger, F., Seifert, F. & Czank, M. (1990). *Eur. J. Mineral.* **2**, 585–594.
- Saburi, S., Kusachi, I., Henmi, C., Kawahara, A., Henmi, K. & Kawada, I. (1976). *Miner. J.* **8**, 240–246.
- Seifert, F., Czank, M., Simons, B. & Schmahl W. (1987). *Phys. Chem. Miner.* **14**, 26–35.
- Warren, B. E. (1930). *Z. Kristallogr.* **74**, 131–138.
- Wolff, P. M. de (1974). *Acta Cryst.* **A30**, 777–785.